Hybrid High-Order methods for Darcean flows in complex porous media

Daniele A. Di Pietro

from joint works with F. Chave and L. Formaggia

Institut Montpelliérain Alexander Grothendieck, University of Montpellier

https://imag.umontpellier.fr/~di-pietro

SimRace2021, 2 December 2021

Geological flows

- Geological flows present a wide panel of mathematical challenges
- Sedimental layers or infrastructures result in complex geometries
- This may additional require adaptive local mesh refinement
- The subsoil is a highly heterogeneous and anisotropic medium
- Faults and fractures can significantly affect flow patterns
- Multiple phases and components can be present
- Flows can induce mechanical deformations on the matrix
- Highly nonlinear behaviours can be present
- ...

References

- Mixed High-Order methods [DP and Ern, 2017]
- Hybrid High-Order methods [DP et al., 2014, DP and Ern, 2015]
- Darcy flows in fractured porous media [Chave, DP, Formaggia, 2018]
- Passive transport in porous media [Chave, DP, Fomaggia, 2019]
- **Introduction to HHO methods [DP and Droniou, 2020]**

Outline

Mixed Darcy problem

- Let $d \geq 2$ and $\mathbb{K} : \Omega \longrightarrow \mathbb{R}^{d\times d}$ be uniformly elliptic
- We seek the velocity $\boldsymbol{u} : \Omega \longrightarrow \mathbb{R}^d$ and the pressure $p : \Omega \longrightarrow \mathbb{R}$ s.t.

$$\begin{aligned} \boldsymbol{u} + \mathbb{K}\,\boldsymbol{\nabla}\, p &= 0 \qquad \text{in } \Omega, \qquad \text{(Darcy's law)} \\ \boldsymbol{\nabla}\cdot \boldsymbol{u} &= f \qquad \text{in } \Omega \qquad \text{(mass balance)} \end{aligned}$$

- The corresponding weak form is: Find $(\boldsymbol{u}, p) \in \boldsymbol{H}(\mathrm{div};\Omega) \times L^2(\Omega)$ s.t.

$$\begin{aligned} m(\boldsymbol{u},\boldsymbol{v}) + b(\boldsymbol{v},p) &= 0 \qquad \forall \boldsymbol{v} \in \boldsymbol{H}(\mathrm{div};\Omega), \\ -b(\boldsymbol{u},q) &= \int_\Omega f\, q \quad \forall q \in L^2(\Omega), \end{aligned}$$

with

$$m(\boldsymbol{u},\boldsymbol{v}) := \int_\Omega \mathbb{K}^{-1}\boldsymbol{u}\cdot\boldsymbol{v}, \qquad b(\boldsymbol{v},q) := -\int_\Omega \boldsymbol{\nabla}\cdot\boldsymbol{v}\, q$$

- **The key dfferential operator is the divergence**

Polytopal meshes

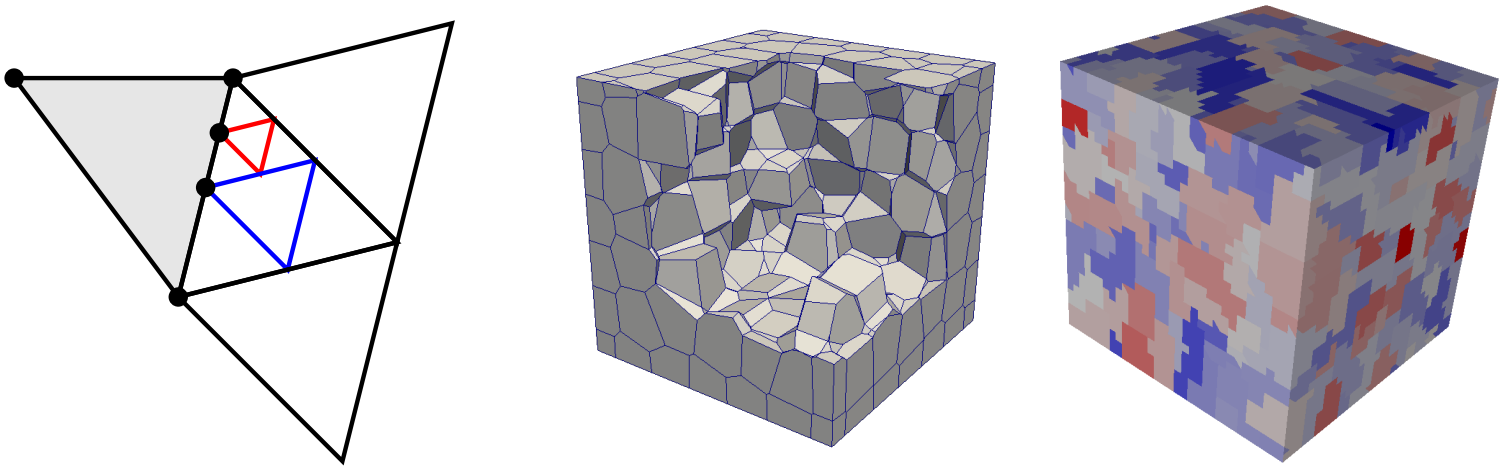

Figure: Examples of polytopal meshes supported by the present approach

Projectors onto local polynomial spaces

- Let $Y \subset \mathbb{R}^d$ be a mesh element/face and $\mathcal{X}$ a subspace of $\mathcal{P}^\ell(Y)$, $\ell \geq 0$
- The L^2-orthogonal projector $\pi^\ell_{\mathcal{X},Y} : L^2(Y) \to \mathcal{X}$ is s.t.

$$\pi^\ell_{\mathcal{X},Y} q = \arg\min_{r \in \mathcal{X}} \|r - q\|^2_{L^2(Y)} \quad \forall q \in L^2(Y)$$

or, equivalently,

$$\int_Y (\pi^\ell_{\mathcal{X},Y} q - q) r = 0 \quad \forall r \in \mathcal{X}$$

- A vector version is defined similarly and denoted in boldface
- We will need, in particular, $\boldsymbol{\pi}^\ell_{\mathcal{G},T}$ with T mesh element and

$$\mathcal{G}^\ell(T) := \nabla \mathcal{P}^{\ell+1}(T)$$

A key remark

- Let $T \in \mathcal{T}_h$ and $\boldsymbol{v} \in H^1(T)^d$. For all $q \in C^\infty(\overline{T})$, it holds

$$\int_T \boldsymbol{\nabla}\cdot \boldsymbol{v}\, q = -\int_T \boldsymbol{v}\cdot\boldsymbol{\nabla} q + \sum_{F\in\mathcal{F}_T}\int_F (\boldsymbol{v}\cdot\boldsymbol{n}_{TF})\, q$$

- Let $k \geq 0$. Specializing this formula to $q \in \mathcal{P}^k(T)$, we can write

$$\int_T \pi^k_{\mathcal{P},T}(\boldsymbol{\nabla}\cdot\boldsymbol{v})\, q = -\int_T \boldsymbol{\pi}^{k-1}_{\mathcal{G},T}\boldsymbol{v}\cdot\boldsymbol{\nabla} q + \sum_{F\in\mathcal{F}_T}\int_F \pi^k_{\mathcal{P},F}(\boldsymbol{v}\cdot\boldsymbol{n}_{TF})\, q$$

- **Hence, $\pi^k_{\mathcal{P},T}(\boldsymbol{\nabla}\cdot\boldsymbol{v})$ is known if $\boldsymbol{\pi}^{k-1}_{\mathcal{G},T}\boldsymbol{v}$ and $(\pi^k_{\mathcal{P},F}(\boldsymbol{v}\cdot\boldsymbol{n}_{TF}))_{F\in\mathcal{F}_T}$ are**

Local discrete space for the velocity

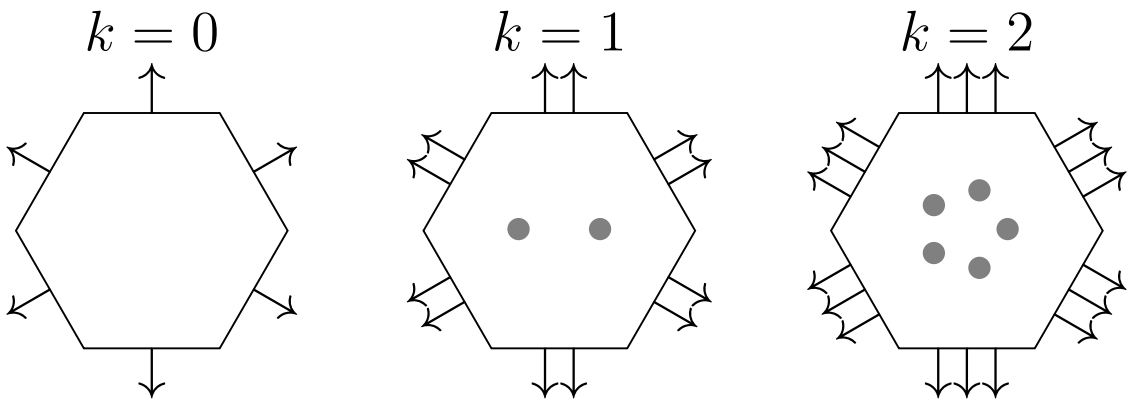

Figure: $\underline{\boldsymbol{U}}_T^k$ for $k \in \{0, 1, 2\}$ and $d = 2$

- For $k \geq 0$ and T mesh element, we define the local MHO space

$$\underline{\boldsymbol{U}}_T^k := \left\{ \underline{\boldsymbol{v}}_T = (\boldsymbol{v}_T, (v_{TF})_{F \in \mathcal{F}_T}) \,:\, \boldsymbol{v}_T \in \boldsymbol{\mathcal{G}}^{k-1}(T),\, v_{TF} \in \mathcal{P}^k(F)\, \forall F \in \mathcal{F}_T \right\}$$

- The corresponding local interpolator $\underline{\boldsymbol{I}}_{\boldsymbol{U},T}^k : H^1(T)^d \to \underline{\boldsymbol{U}}_T^k$ is s.t.

$$\underline{\boldsymbol{I}}_{\boldsymbol{U},T}^k \boldsymbol{v} := (\boldsymbol{\pi}_{\boldsymbol{\mathcal{G}},T}^{k-1} \boldsymbol{v}, \pi_{\mathcal{P},F}^k (\boldsymbol{v} \cdot \boldsymbol{n}_{TF}))$$

Reconstructions I

- The local discrete divergence $D_T^k : \underline{\boldsymbol{U}}_T^k \to \mathcal{P}^k(T)$ is s.t.

$$\int_T D_T^k \underline{\boldsymbol{v}}_T \, q = -\int_T \boldsymbol{v}_T \cdot \boldsymbol{\nabla} q + \sum_{F \in \mathcal{F}_T} \int_F v_{TF} \, q \quad \forall q \in \mathcal{P}^k(T)$$

- By construction, the following commutative diagram holds:

$$\begin{array}{ccc} H^1(T)^d & \xrightarrow{\boldsymbol{\nabla}\cdot} & L^2(T) \\ \downarrow{\scriptstyle \underline{\boldsymbol{I}}_{\boldsymbol{U},T}^k} & & \downarrow{\scriptstyle \pi_{\mathcal{P},T}^k} \\ \underline{\boldsymbol{U}}_T^k & \xrightarrow{D_T^k} & \mathcal{P}^k(T) \end{array}$$

- **This is a key property in Fortin's argument for stability**

Reconstructions II

- For simplicity, assume $\mathbb{K}$ piecewise constant on the mesh $\mathcal{T}_h$
- The local discrete velocity $\boldsymbol{P}_T^k : \underline{\boldsymbol{U}}_T^k \to \mathbb{K}_{|T}\boldsymbol{\mathcal{G}}^k(T)$ is s.t.

$$\int_T \boldsymbol{P}_T^k \underline{\boldsymbol{v}}_T \cdot \boldsymbol{\nabla} q = -\int_T D_T^k \underline{\boldsymbol{v}}_T \, q + \sum_{F \in \mathcal{F}_T} \int_F v_{TF} \, q \quad \forall q \in \mathcal{P}^{k+1}(T)$$

- By construction, we have the following polynomial consistency property

$$\boldsymbol{P}_T^k(\underline{\boldsymbol{I}}_{\boldsymbol{U},T}^k \boldsymbol{v}) = \boldsymbol{v} \qquad \forall \boldsymbol{v} \in \mathbb{K}_{|T}\boldsymbol{\mathcal{G}}^k(T)$$

or, equivalently,

$$\boldsymbol{P}_T^k[\underline{\boldsymbol{I}}_{\boldsymbol{U},T}^k(\mathbb{K}_{|T}\boldsymbol{\nabla} q)] = \boldsymbol{\nabla} q \qquad \forall q \in \mathcal{P}^{k+1}(T)$$

Local weighted L^2-product

- We define the discrete weighted L^2-product of velocities as

$$(\underline{\boldsymbol{w}}_T, \underline{\boldsymbol{v}}_T)_{\boldsymbol{U},T} := \int_T \mathbb{K}_{|T}^{-1} \boldsymbol{P}_T^k \underline{\boldsymbol{w}}_T \cdot \boldsymbol{P}_T^k \underline{\boldsymbol{v}}_T + s_{\boldsymbol{U},T}(\underline{\boldsymbol{w}}_T, \underline{\boldsymbol{v}}_T),$$

  where, with $K_{TF} := \boldsymbol{n}_{TF}^\top \mathbb{K}_{|T} \boldsymbol{n}_{TF}$, the stabilization bilinear form is s.t.

$$s_{\boldsymbol{U},T}(\underline{\boldsymbol{w}}_T, \underline{\boldsymbol{v}}_T) := \sum_{F \in \mathcal{F}_T} \frac{h_F}{K_{TF}} \int_F (\boldsymbol{P}_T^k \underline{\boldsymbol{w}}_T \cdot \boldsymbol{n}_{TF} - w_{TF})(\boldsymbol{P}_T^k \underline{\boldsymbol{v}}_T \cdot \boldsymbol{n}_{TF} - v_{TF})$$

- This choice satisfies, for all $(q, \underline{\boldsymbol{v}}_T) \in \mathcal{P}^{k+1}(T) \times \underline{\boldsymbol{U}}_T^k$,

$$s_{\boldsymbol{U},T}(\underline{\boldsymbol{I}}_T^k(\mathbb{K}_{|T} \boldsymbol{\nabla} q), \underline{\boldsymbol{v}}_T) = 0$$

Global velocity space, divergence, and L^2-product

- The global velocity space mimicks the continuity of normal velocities
- Specifically, we set

$$\underline{\boldsymbol{U}}_h^k := \Big\{ \underline{\boldsymbol{v}}_h = (\underline{\boldsymbol{v}}_T)_{T\in\mathcal{T}_h} \ : \ \underline{\boldsymbol{v}}_T \in \underline{\boldsymbol{U}}_T^k \text{ for all } T \in \mathcal{T}_h \\ \text{and } v_{T_1F} + v_{T_2F} = 0 \text{ for any interface } F \subset \partial T_1 \cap \partial T_2 \Big\}$$

- A global divergence reconstruction is obtained setting

$$(D_h^k \underline{\boldsymbol{v}}_h)_{|T} := D_T^k \underline{\boldsymbol{v}}_T \qquad \forall T \in \mathcal{T}_h$$

- The global L^2-product is assembled from local contributions:

$$(\underline{\boldsymbol{w}}_h, \underline{\boldsymbol{v}}_h)_{\boldsymbol{U},h} := \sum_{T\in\mathcal{T}_h} (\underline{\boldsymbol{w}}_T, \underline{\boldsymbol{v}}_T)_{\boldsymbol{U},T}$$

A Mixed High-Order method

- Recall the continuous problem: Find $(\boldsymbol{u}, p) \in \boldsymbol{H}(\mathrm{div};\Omega) \times L^2(\Omega)$ s.t.

$$\begin{aligned} m(\boldsymbol{u},\boldsymbol{v}) + b(\boldsymbol{v},p) &= 0 && \forall \boldsymbol{v} \in \boldsymbol{H}(\mathrm{div};\Omega), \\ -b(\boldsymbol{u},q) &= \int_\Omega f\, q && \forall q \in L^2(\Omega) \end{aligned}$$

- The discrete problem reads: Find $(\underline{\boldsymbol{u}}_h, p_h) \in \underline{\boldsymbol{U}}_h^k \times \mathcal{P}^k(\mathcal{T}_h)$ s.t.

$$\begin{aligned} m_h(\underline{\boldsymbol{u}}_h,\underline{\boldsymbol{v}}_h) + b_h(\underline{\boldsymbol{v}}_h,p_h) &= 0 && \forall \underline{\boldsymbol{v}}_h \in \underline{\boldsymbol{U}}_h^k, \\ -b_h(\underline{\boldsymbol{u}}_h,q_h) &= \int_\Omega f\, q_h && \forall q_h \in \mathcal{P}^k(\mathcal{T}_h), \end{aligned}$$

with

$$m_h(\underline{\boldsymbol{u}}_h,\underline{\boldsymbol{v}}_h) \coloneqq (\underline{\boldsymbol{w}}_h,\underline{\boldsymbol{v}}_h)_{\boldsymbol{U},h}, \quad b_h(\underline{\boldsymbol{v}}_h,q_h) \coloneqq -\int_\Omega D_h^k \underline{\boldsymbol{v}}_h\, q_h$$

Error estimates I

Theorem (Basic error estimate)

Under the additional regularity $p \in H^{k+2}(\mathcal{T}_h)$, *it holds*

$$\|\underline{\boldsymbol{I}}_h^k \boldsymbol{u} - \underline{\boldsymbol{u}}_h\|_{\boldsymbol{U},h} + \|\pi_{\mathcal{P},h}^k p - p_h\|_{L^2(\Omega)} \lesssim \left(\sum_{T \in \mathcal{T}_h} \rho_T \, \overline{K}_T \, h_T^{2(k+1)} |p|^2_{H^{k+2}(T)} \right)^{1/2}$$

with $\|\cdot\|_{\boldsymbol{U},h}$ *norm induced by* $(\cdot,\cdot)_{\boldsymbol{U},h}$ *on* $\underline{\boldsymbol{U}}_h$, *local anisotropy ratio*

$$\rho_T := \frac{\overline{K}_T}{\underline{K}_T},$$

and $\underline{K}_T$, $\overline{K}_T$ *respectively the smallest and largest eigenvalue of* $\mathbb{K}_{|T}$ *for any mesh element* $T \in \mathcal{T}_h$.

Error estimates II

Theorem (Superconvergence of the pressure)

Under elliptic regularity (which requires $\mathbb{K}$ constant on Ω), and further assuming $f \in H^1(\Omega)$ if $k = 0$,

$$\|\pi^k_{\mathcal{P},h} p - p_h\|_{L^2(\Omega)} \lesssim \begin{cases} h^2 \|f\|_{H^1(\Omega)} & \text{if } k = 0, \\ h^{k+2} |p|_{H^{k+2}(\mathcal{T}_h)} & \text{if } k \geq 1. \end{cases}$$

Numerical examples I

- We consider the manufactured solution

$$p(x,y) = 2\sin(\pi x)\sin(\pi y) \text{ with } \mathbb{K} = \begin{pmatrix} 1 & 0 \\ 0 & \rho^{-1} \end{pmatrix}$$

- We assess convergence rates and robustness with respect to anisotropy

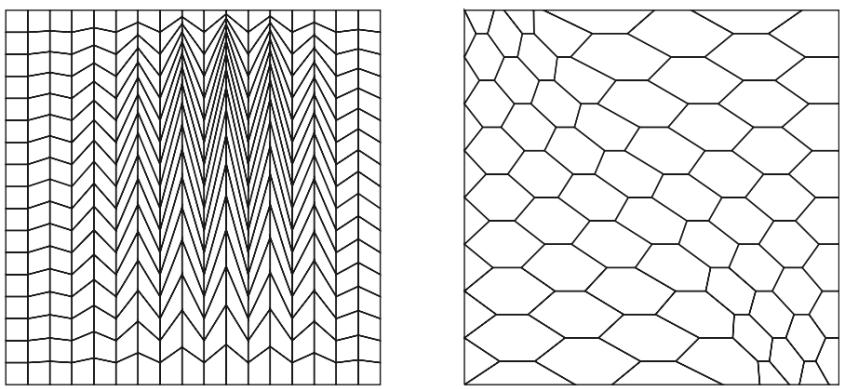

Figure: Kershaw and hexagonal meshes used in the numerical test case

Numerical examples II

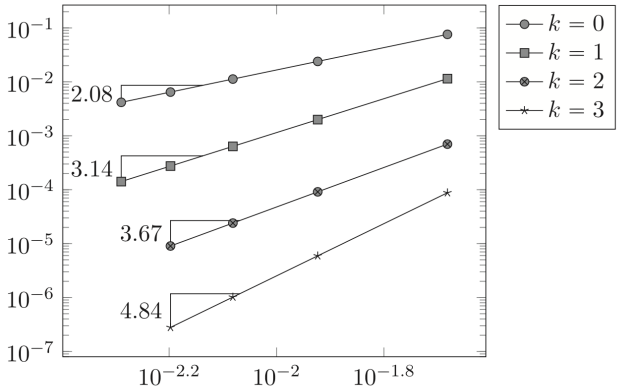

(c) $\|\widehat{\underline{\boldsymbol{\sigma}}}_h - \underline{\boldsymbol{\sigma}}_h\|_H$ vs. h, Kershaw mesh

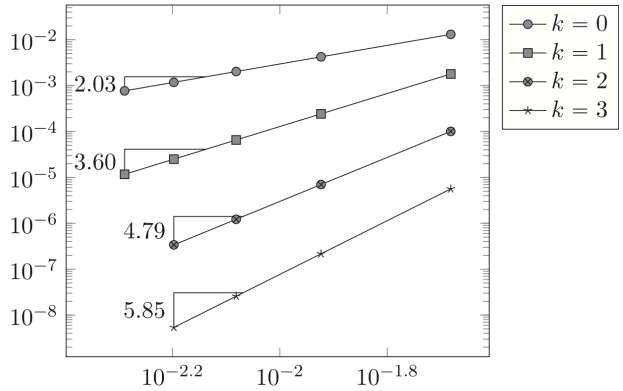

(d) $\|\widehat{u}_h - u_h\|$ vs. h, Kershaw mesh

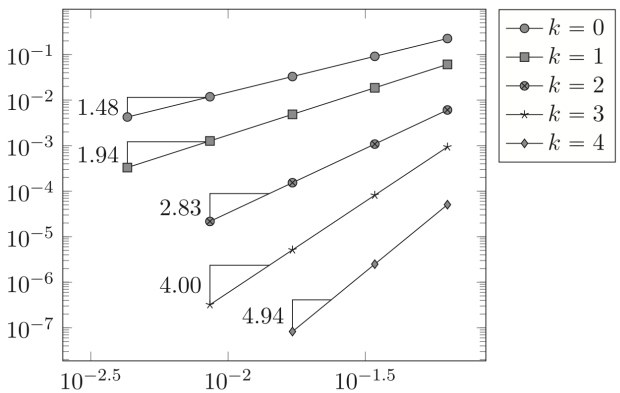

(e) $\|\widehat{\underline{\boldsymbol{\sigma}}}_h - \underline{\boldsymbol{\sigma}}_h\|_H$ vs. h, hexagonal mesh

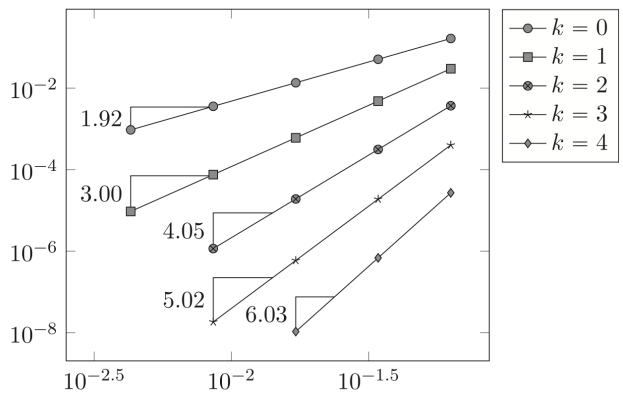

(f) $\|\widehat{u}_h - u_h\|$ vs. h, hexagonal meshes

Figure: Flux (left) and pressure (right) convergence for the MHO method on Kershaw (top) and hexagonal meshes (bottom)

Numerical examples III

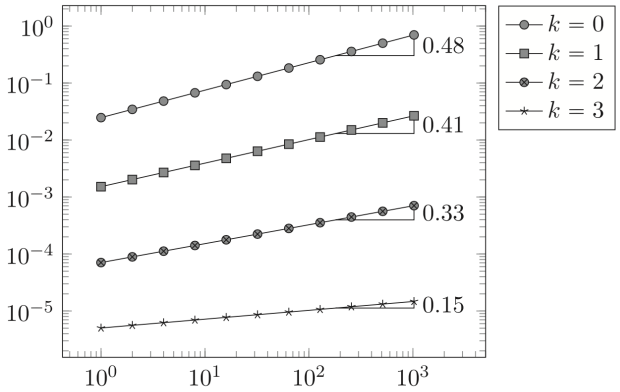

(c) $\|\underline{\widehat{\boldsymbol{\sigma}}}_h - \underline{\boldsymbol{\sigma}}_h\|_H$ vs. $\rho_{\mathbf{K}}$, Kershaw mesh

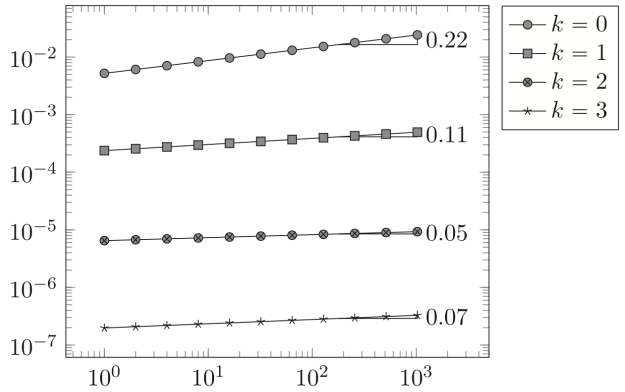

(d) $\|\widehat{u}_h - u_h\|$ vs. $\rho_{\mathbf{K}}$, Kershaw mesh

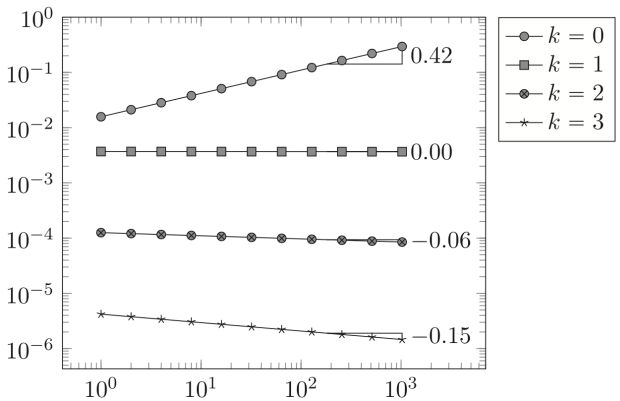

(e) $\|\underline{\widehat{\boldsymbol{\sigma}}}_h - \underline{\boldsymbol{\sigma}}_h\|_H$ vs. $\rho_{\mathbf{K}}$, hexagonal mesh

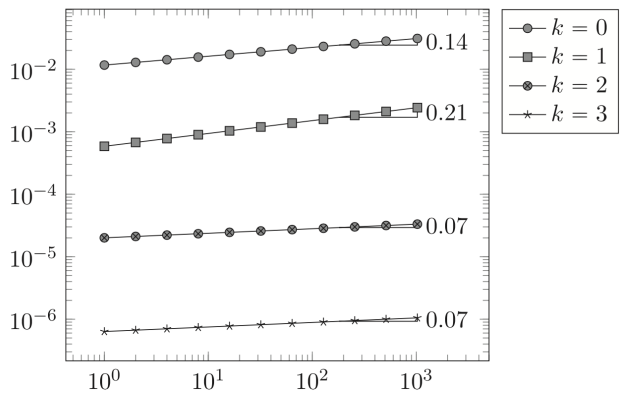

(f) $\|\widehat{u}_h - u_h\|$ vs. $\rho_{\mathbf{K}}$, hexagonal mesh

Figure: Robustness of the MHO method with respect the anisotropy for the flux (left) and pressure (right) on Kershaw (top) and hexagonal meshes (bottom)

Outline

A simplified model problem I

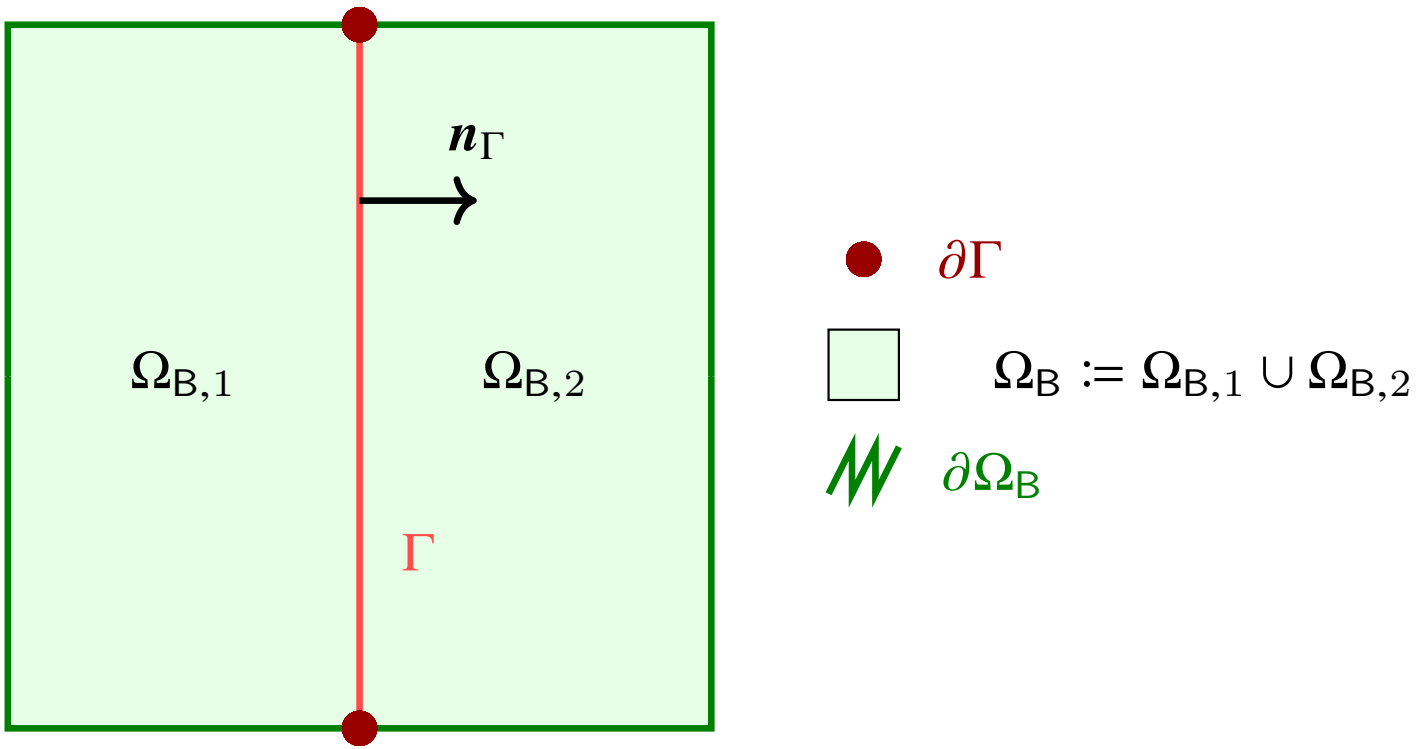

Figure: A simplified two-dimensional configuration

Governing equations

- In the bulk, we consider again the Darcy equation in mixed form:

$$\boldsymbol{u} + \mathbb{K}\,\boldsymbol{\nabla}\,p = 0 \text{ and } \boldsymbol{\nabla}\cdot\boldsymbol{u} = f \text{ in } \Omega_{\mathsf{B}}$$

- Flow in the fracture is also governed by Darcy, this time in primal form:

$$-\boldsymbol{\nabla}_\Gamma\cdot(K_\Gamma\,\boldsymbol{\nabla}_\Gamma\,p^\Gamma) = \ell_\Gamma f_\Gamma + [\![\boldsymbol{u}]\!]_\Gamma\cdot\boldsymbol{n}_\Gamma \quad \text{in } \Gamma,$$

  where $K_\Gamma := \kappa_\Gamma^{\boldsymbol{t}}\ell_\Gamma$ with $\kappa_\Gamma^{\boldsymbol{t}}$ tangential permeability and ℓ_Γ fracture width

- Finally, we consider the following coupling conditions:

$$\lambda_\Gamma\{\boldsymbol{u}\}_\Gamma\cdot\boldsymbol{n}_\Gamma = [\![p]\!]_\Gamma \text{ and } \lambda_\Gamma^\xi[\![\boldsymbol{u}]\!]_\Gamma\cdot\boldsymbol{n}_\Gamma = \{p\}_\Gamma - p^\Gamma \text{ on } \Gamma$$

  with $\xi \in \left(\frac{1}{2}, 1\right]$ model parameter, $\lambda_\Gamma := \frac{\ell_\Gamma}{\kappa_\Gamma^{\boldsymbol{n}}}$, and $\lambda_\Gamma^\xi := \lambda_\Gamma\left(\frac{\xi}{2} - \frac{1}{4}\right)$

- The model is completed with bulk and fracture boundary conditions

Discretization

- In the bulk, we use the MHO method described above
- In the fracture, we use the standard (primal) HHO method
- All quantities appearing in the coupling conditions are naturally available with this choice

Fracture flow I

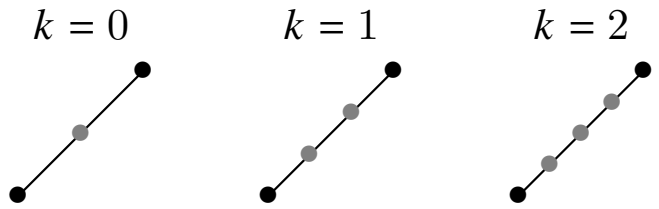

Figure: Local hybrid space of discrete unknowns $\underline{P}^k_{\Gamma,F}$ for $F \in \mathcal{F}_h^\Gamma$ and $k \in \{0, 1, 2\}$

- The space of fracture pressure unknowns is

$$\underline{P}^k_{\Gamma,h} \coloneqq \Big\{ \underline{q}^\Gamma_F = \big((q^\Gamma_F)_{F\in\mathcal{F}_h^\Gamma}, (q^\Gamma_V)_{V\in\mathcal{V}_h^\Gamma}\big) : q^\Gamma_F \in \mathcal{P}^k(F) \text{ for all } F \in \mathcal{F}_h^\Gamma \text{ and } q^\Gamma_V \in \mathbb{R} \text{ for all } V \in \mathcal{V}_h^\Gamma \Big\}$$

- The corresponding interpolator $\underline{I}^k_{\Gamma,h} : H^1(\Omega) \to \underline{P}_{\Gamma,h}$ is

$$\underline{I}^k_{\Gamma,h} q \coloneqq \big((\pi^k_{\mathcal{P},F} q_{|F})_{\mathcal{F}_h^\Gamma}, (q(\boldsymbol{x}_V))_{V\in\mathcal{V}_h^\Gamma}\big)$$

- Their restrictions to $F \in \mathcal{F}_h^\Gamma$ are denoted by $\underline{P}^k_{\Gamma,F}$ and $\underline{I}^k_{\Gamma,F}$

Fracture flow II

- For $F \in \mathcal{F}_h^\Gamma$, the pressure reconstruction $r_F^{k+1} : \underline{P}_{\Gamma,F}^k \to \mathcal{P}^{k+1}(F)$ is s.t.

$$\int_F \boldsymbol{\nabla}_\Gamma r_F^{k+1} \underline{q}_F^\Gamma \cdot \boldsymbol{\nabla}_\Gamma w + \int_F r_F^{k+1} \underline{q}_F^\Gamma \times \int_F w$$
$$= -\int_F q_F^\Gamma \, \Delta_\Gamma w + \sum_{V \in \mathcal{V}_F} q_V^\Gamma \, (\boldsymbol{\nabla}_\Gamma w(\boldsymbol{x}_V) \cdot \boldsymbol{t}_{FV}) + \int_F q_F^\Gamma \times \int_F w$$

- $a_h : \underline{P}_{\Gamma,h}^k \times \underline{P}_{\Gamma,h}^k \to \mathbb{R}$ is assembled from the local contributions

$$a_F(\underline{p}_F^\Gamma, \underline{q}_F^\Gamma) := \int_F K_F \, \boldsymbol{\nabla}_\Gamma r_F^{k+1} \underline{p}_F^\Gamma \cdot \boldsymbol{\nabla}_\Gamma r_F^{k+1} \underline{q}_F^\Gamma + s_{P,F}(\underline{p}_F^\Gamma, \underline{q}_F^\Gamma)$$

- $\underline{P}_{\Gamma,h,0}^k$ incorporates the homogeneous Dirichlet b.c. at fracture tips

Discrete problem

The discrete problem reads: Find $(\underline{\boldsymbol{u}}_h, p_h, \underline{p}_h^\Gamma) \in \underline{\boldsymbol{U}}_h^k \times \mathcal{P}^k(\mathcal{T}_h) \times \underline{P}_{\Gamma,h,0}^k$ s.t.

$$
\begin{aligned}
m_h(\underline{\boldsymbol{u}}_h, \underline{\boldsymbol{v}}_h) + c_h(\underline{\boldsymbol{u}}_h, \underline{\boldsymbol{v}}_h) + b_h(\underline{\boldsymbol{v}}_h, p_h) + b_h^\Gamma(\underline{\boldsymbol{v}}_h, \underline{p}_h^\Gamma) &= 0 && \forall \underline{\boldsymbol{v}}_h \in \underline{\boldsymbol{U}}_h^k, \\
-b_h(\underline{\boldsymbol{u}}_h, q_h) &= \int_{\Omega_B} f q_h && \forall q_h \in \mathcal{P}^k(\mathcal{T}_h), \\
-b_h^\Gamma(\underline{\boldsymbol{u}}_h, \underline{q}_h^\Gamma) + a_h(\underline{p}_h^\Gamma, \underline{q}_h^\Gamma) &= \int_\Gamma \ell_\Gamma f_\Gamma q_h^\Gamma && \forall \underline{q}_h^\Gamma \in \underline{P}_{\Gamma,h,0}^k
\end{aligned}
$$

with bilinear forms $b_h^\Gamma : \underline{\boldsymbol{U}}_h^k \times \underline{P}_{\Gamma,h,0}^k \to \mathbb{R}$ and $c_h : \underline{\boldsymbol{U}}_h^k \times \underline{\boldsymbol{U}}_h^k \to \mathbb{R}$ s.t.

$$
b_h^\Gamma(\underline{\boldsymbol{v}}_h, \underline{q}_h^\Gamma) \coloneqq \sum_{F \in \mathcal{F}_h^\Gamma} \int_F [\![\underline{\boldsymbol{v}}_h]\!]_F \, q_F^\Gamma,
$$

$$
c_h(\underline{\boldsymbol{u}}_h, \underline{\boldsymbol{v}}_h) \coloneqq \sum_{F \in \mathcal{F}_h^\Gamma} \int_F \left(\lambda_F^\xi [\![\underline{\boldsymbol{u}}_h]\!]_F [\![\underline{\boldsymbol{v}}_h]\!]_F + \lambda_F \{\underline{\boldsymbol{u}}_h\}_F \{\underline{\boldsymbol{v}}_h\}_F \right)
$$

Error estimate

Theorem (Error estimate)

Define the following norm on $\underline{\boldsymbol{U}}_h^k$*:*

$$\|\underline{\boldsymbol{v}}_h\|_{\boldsymbol{U},\xi,h} \coloneqq \left(m_h(\underline{\boldsymbol{v}}_h,\underline{\boldsymbol{v}}_h) + c_h(\underline{\boldsymbol{v}}_h,\underline{\boldsymbol{v}}_h)\right)^{\frac{1}{2}}.$$

Then, denoting by $\|\cdot\|_{\Gamma,h}$ *the standard component* H^1*-like HHO norm, and assuming the additional regularity* $p \in H^{k+2}(\mathcal{T}_h)$ *and* $p^\Gamma \in H^{k+2}(\mathcal{F}_h^\Gamma)$*,*

$$\begin{aligned}&\|\underline{\boldsymbol{u}}_h - \underline{\boldsymbol{I}}_h^k \boldsymbol{u}\|_{\boldsymbol{U},h} + \chi\|p_h - \pi_{\mathcal{P},h}^k p\|_{L^2(\Omega)} + \|\underline{p}_h^\Gamma - \underline{I}_{\Gamma,h}^k p^\Gamma\|_{\Gamma,h}\\ &\quad\lesssim \left(\sum_{T\in\mathcal{T}_h} \rho_T \overline{K}_T h_T^{2(k+1)} \|p\|_{H^{k+2}(T)}^2 + \sum_{F\in\mathcal{F}_h^\Gamma} K_{\Gamma|F} h_F^{2(k+1)} \|p^\Gamma\|_{H^{k+2}(F)}^2\right),\end{aligned}$$

with χ *independent of* h *but possibly depending on* $\rho \coloneqq \max_{T\in\mathcal{T}_h} \rho_T$*,* k*, and on the problem geometry and data.*

Assessment of the convergence rates I

Take $\Omega_B := (0,1)^2 \setminus \overline{\Gamma}$, $\Gamma := \{0.5\} \times (0,1)$, and f, f^Γ and b.c. s.t.

$$p(\boldsymbol{x}) := \begin{cases} \sin(4x_1)\cos(\pi x_2) & \text{if } x_1 < 0.5, \\ \cos(4x_1)\cos(\pi x_2) & \text{if } x_1 > 0.5, \end{cases}$$

$$p^\Gamma(\boldsymbol{x}) := \xi(\cos(2) + \sin(2))\cos(\pi x_2),$$

with $\ell_\Gamma = 0.01$, $\xi = 0.75$, $\kappa_\Gamma^n \in \{1, 2\ell_\Gamma\}$, $\kappa_\Gamma^\tau = 1$, and $\mathbb{K} = \begin{pmatrix} \kappa_\Gamma^n/2\ell_\Gamma & 0 \\ 0 & 1 \end{pmatrix}$

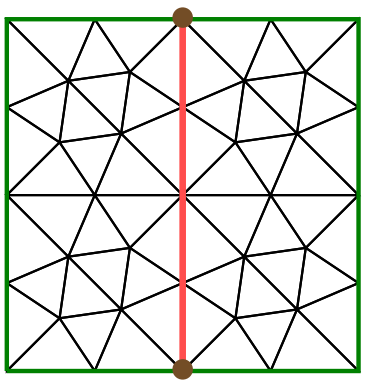

(a) Triangular

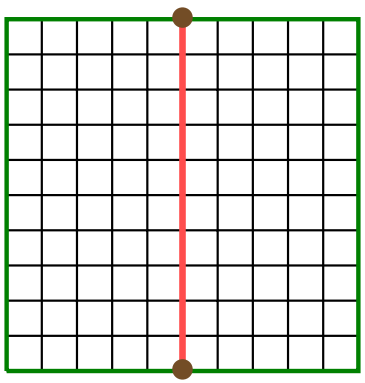

(b) Cartesian

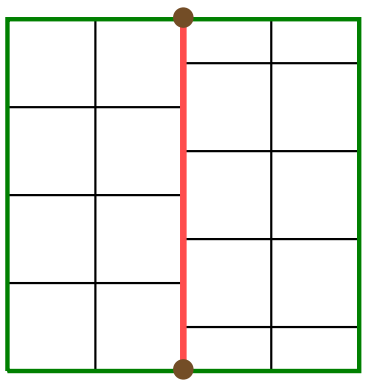

(c) Nonconforming

Assessment of the convergence rates II

Figure: Meshes used in the numerical test case

Assessment of the convergence rates III

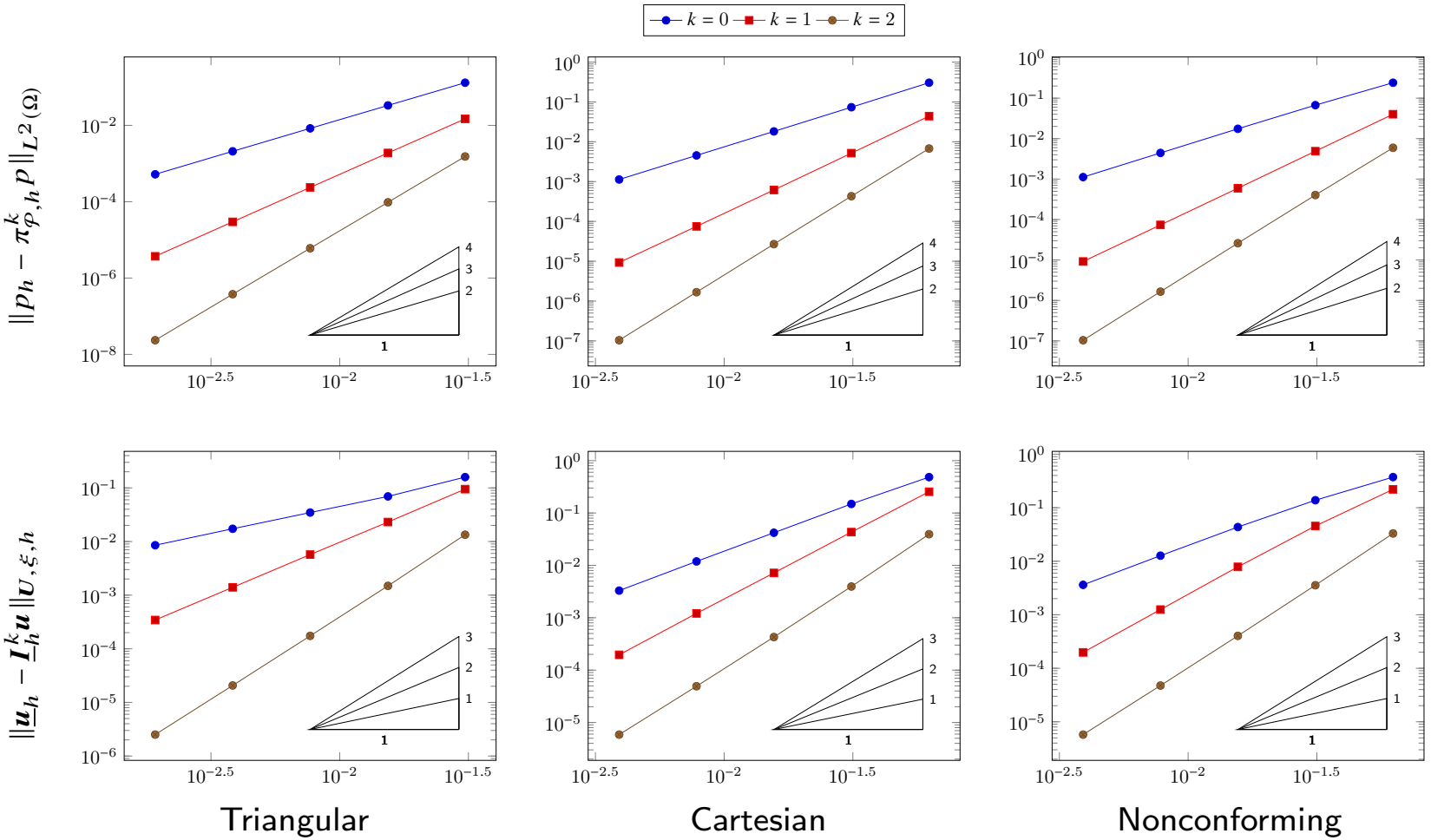

Figure: Errors vs. h (bulk), $\dfrac{\overline{K}_{\mathrm{B}}}{\underline{K}_{\mathrm{B}}} = 1$

Assessment of the convergence rates IV

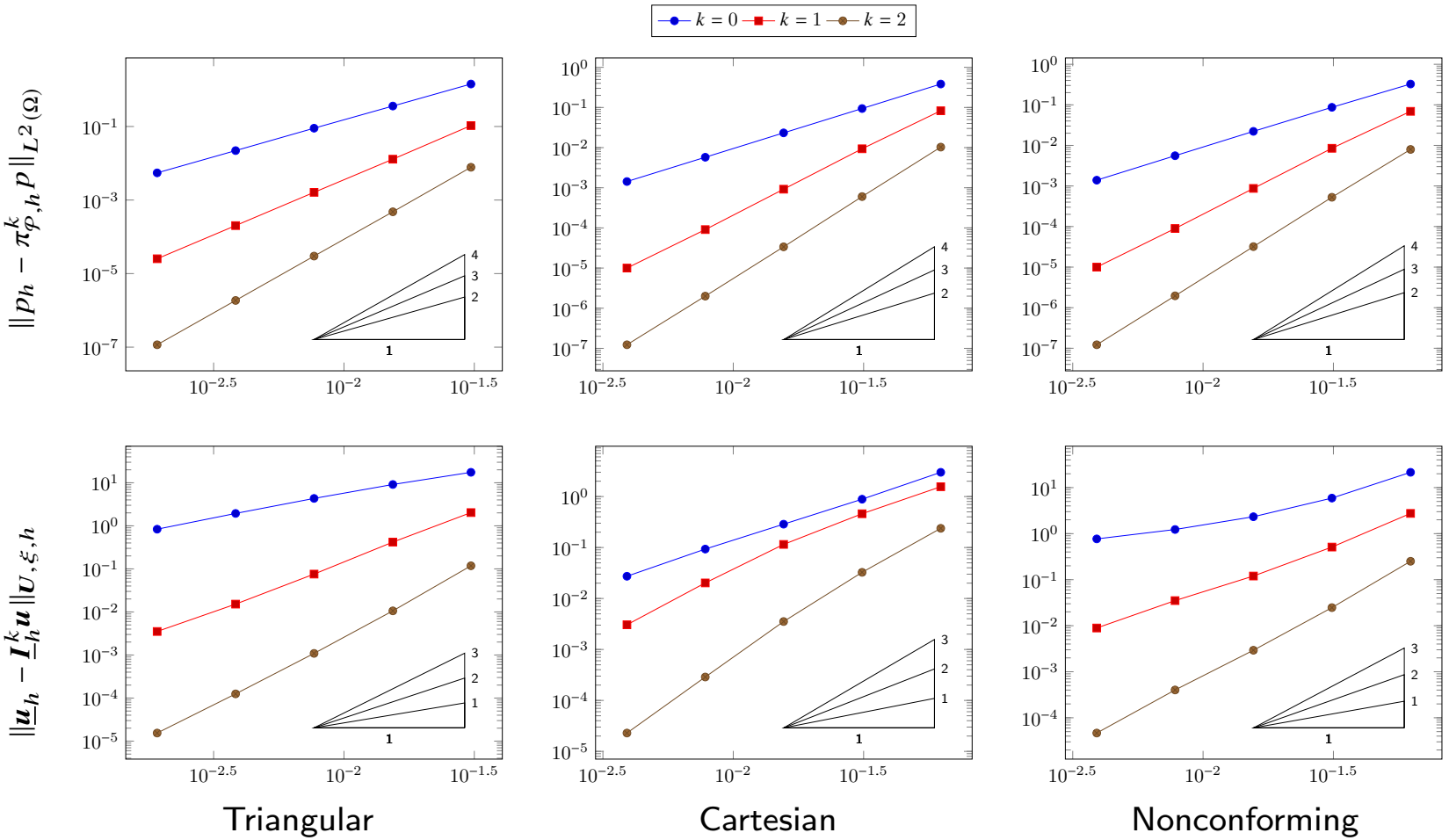

Figure: Errors vs. h (bulk), $\dfrac{\overline{K}_{\mathsf{B}}}{\underline{K}_{\mathsf{B}}} = 50$

Assessment of the convergence rates V

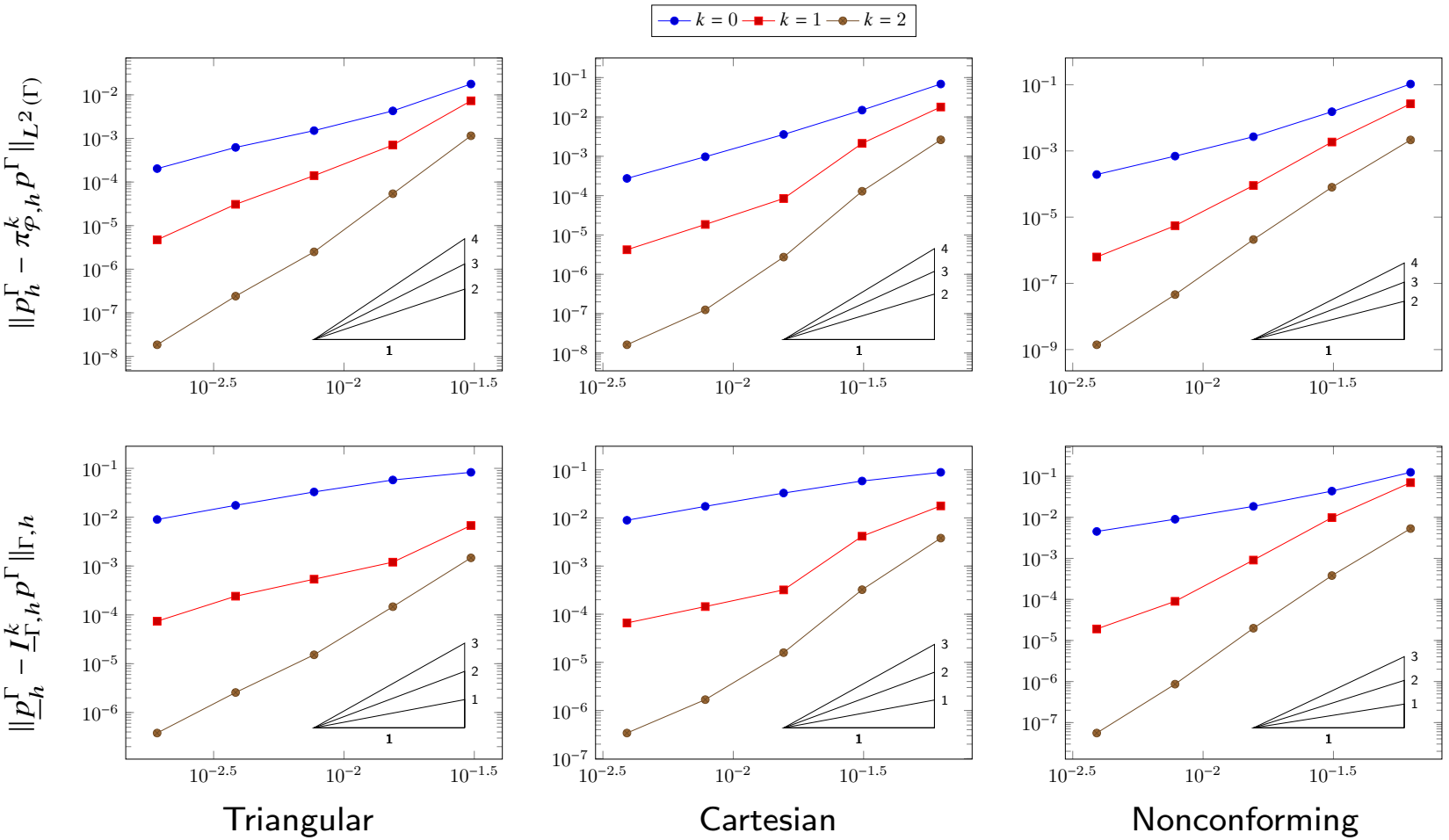

Figure: Errors vs. h (fracture), $\dfrac{\overline{K}_\mathrm{B}}{\underline{K}_\mathrm{B}} = 1$

Assessment of the convergence rates VI

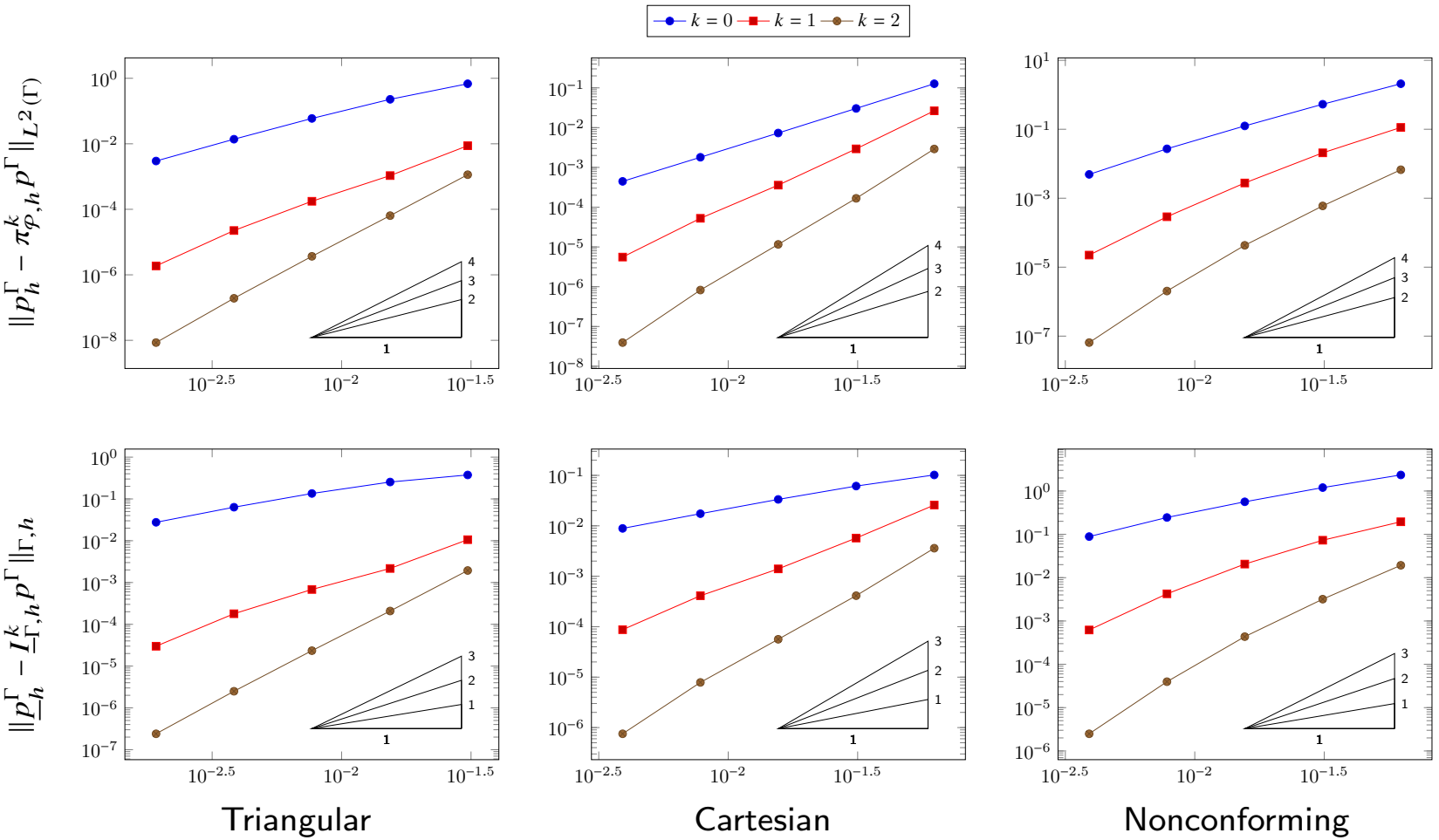

Figure: Errors vs. h (fracture), $\dfrac{\overline{K}_\mathrm{B}}{\underline{K}_\mathrm{B}} = 50$

References

Chave, F., Di Pietro, D. A., and Formaggia, L. (2018).

A Hybrid High-Order method for Darcy flows in fractured porous media.
SIAM J. Sci. Comput., 40(2):A1063–A1094.

Chave, F., Di Pietro, D. A., and Formaggia, L. (2019).

A Hybrid High-Order method for passive transport in fractured porous media.
Int. J. Geomath., 10(12).

Di Pietro, D. A. and Droniou, J. (2020).

The Hybrid High-Order method for polytopal meshes, volume 19 of *Modeling, Simulation and Application*.
Springer International Publishing.

Di Pietro, D. A. and Ern, A. (2015).

A hybrid high-order locking-free method for linear elasticity on general meshes.
Comput. Meth. Appl. Mech. Engrg., 283:1–21.

Di Pietro, D. A. and Ern, A. (2017).

Arbitrary-order mixed methods for heterogeneous anisotropic diffusion on general meshes.
IMA J. Numer. Anal., 37(1):40–63.

Di Pietro, D. A., Ern, A., and Lemaire, S. (2014).

An arbitrary-order and compact-stencil discretization of diffusion on general meshes based on local reconstruction operators.
Comput. Meth. Appl. Math., 14(4):461–472.
Open access (editor's choice).